Artificial Intelligence in Medicine 78 (2017) 1–13

Contents lists available at ScienceDirect

Artificial Intelligence in Medicine

journal homepage: www.elsevier.com/locate/aiim

Modeling new immunoregulatory therapeutics as antimicrobial alternatives for treating *Clostridium difficile* infection

Andrew Leber, Raquel Hontecillas, Vida Abedi, Nuria Tubau-Juni, Victoria Zoccoli-Rodriguez, Caroline Stewart, Josep Bassaganya-Riera *

Nutritional Immunology and Molecular Medicine Laboratory[1], *Biocomplexity Institute, Virginia Tech, Blacksburg, VA, United States*

ARTICLE INFO

Article history:
Received 27 December 2016
Received in revised form 6 March 2017
Accepted 6 May 2017

Keywords:
Clostridium difficile
In silico clinical trials
Gastrointestinal disease modeling
LANCL2
Immunoregulation

ABSTRACT

The current treatment paradigm in *Clostridium difficile* infection is the administration of antibiotics contributing to the high rates of recurrent infections. Recent alternative strategies, such as fecal microbiome transplantation and anti-toxin antibodies, have shown similar efficacy in the treatment of *C. difficile* associated disease (CDAD). However, barriers exist for either treatment or other novel treatments to displace antibiotics as the standard of care. To aid in the comparison of these and future treatments in CDAD, we developed an *in silico* pipeline to predict clinical efficacy with nonclinical results. The pipeline combines an ordinary differential equation (ODE)-based model, describing the immunological and microbial interactions in the gastrointestinal (GI) mucosa, with machine learning algorithms to translate simulated output quantities (i.e. time of clearance, quantity of commensal bacteria, T cell ratios) into clinical predictions based on prior preclinical, translational and clinical trial data. As a use case, we compare the efficacy of lanthionine synthetase C-like 2 (LANCL2), a novel immunoregulatory target with promising efficacy in inflammatory bowel disease (IBD), activation with antibiotics, fecal microbiome transplantation and anti-toxin antibodies in the treatment of CDAD. We further validate the potential of LANCL2 pathway activation, in a mouse model of *C. difficile* infection in which it displays an ability to decrease weight loss and inflammatory cell types while protecting against mortality. The computational pipeline can serve as an important resource in the development of new treatment modalities.

1. Introduction

Clostridium difficile is an anaerobic bacterium that relies on opportunistic colonization or expansion following antibiotic-related disruptions of the gut microbiome. The associated infections are responsible for an estimated 450,000 cases and 29,000 deaths per year in the United States [1]. *C. difficile* infections (CDI) have considerable rates of recurrence, ranging between 20 and 25% depending on the estimate, due to further treatment with antibiotics to kill the pathogen [1–3]. Further, the incidence of CDI continues to rise, more than doubling its share of hospitalization stays from 2000 to 2009, potentially due to the emergence of hyper-virulent and antibiotic resistant strains [4]. Also contributing to the continued suppression of commensal bacteria may be the production of antimicrobial peptides from activated immune cells and inflamed epithelial cells [5]. Together, these factors may perpetuate the original microbial environment, allowing residual *C. difficile* to re-expand following the cessation of treatment. Therefore, new strategies must be developed to effectively reduce the severity of disease while also limiting the rates of recurrence.

Currently, the recommended treatment regimen for mild, severe, and recurrent CDI is antibiotic therapy based on the belief that to cure disease the pathogen must be removed [6,7]. However, the clinical outcomes and associated pathologies of CDI correlate more with markers of intestinal inflammation than markers of *C. difficile* burden [8]. Recent advances in CDI treatment led to the development of alternative strategies that modulate the commensal microbiome, such as fecal microbiome transplantation or administration of non-toxigenic *C. difficile*, or directly influence the capability of *C. difficile* to induce inflammation, such as anti-toxin A and B antibodies [9–11]. The success of these alternative treatments suggests that development of therapeutics with similar effect profiles, such as those targeting the activation of immunoregulatory pathways, may find similar efficacy.

Among the immunoregulatory pathways that may offer promise in the treatment of enteric pathogens like *C. difficile* is the LANCL2

* Corresponding author.
E-mail address: jbassaga@vt.edu (J. Bassaganya-Riera).
[1] www.nimml.org.

http://dx.doi.org/10.1016/j.artmed.2017.05.003
0933-3657/

pathway. LANCL2 was first recognized as a mammalian receptor for abscisic acid (ABA) [12]. Downstream effects of LANCL2 and ABA have shown broad anti-inflammatory and metabolic activity including modulation of calcium-dependent, glucose transport, and Akt pathways as well as the downregulation of inflammatory markers [12–14]. Recently, a novel class of bis-(benzimidazolyl)-terephthalanilides (BTTs) has been discovered to bind to LANCL2 and promote beneficial effects in the context of inflammatory bowel disease [15], the properties of which have been optimized [16] and assessed for toxicity [17]. As a result, we seek to assess the ability of NSC61610, a BTT, to reduce CDAD as an alternative to antibiotic therapy.

However, the need to co-administer standard of care antibiotics in addition to alternative therapeutics, designed to in part promote commensal preservation, in clinical trial settings may lessen their impact [18]. Additionally, while important for the understanding of disease progression and pathologies, the ability of animal models to independently predict the effectiveness of *C. difficile* treatments is questionable [19]. Notably, in animal trials of anti-toxin antibodies, the majority of the effectiveness was shown to be through anti-Toxin A antibodies [20]. The anti-Toxin B antibodies were thought to have little to no independent effect. When these trials moved into the clinical setting, the treatment efficacy was shown to be almost entirely dependent on the presence of anti-Toxin B antibodies [10,21].

Recently, *in silico* clinical trials (ISCTs) have been developed for the nonclinical assessment of novel treatments for tuberculosis, type 1 diabetes, and traumatic injury, among others [22–24]. These ISCTs vary in complexity and design but retain the same underlying principles: a computational model or simulation method to maintain mechanistic realism, the generation of virtual patients with artificial variation in behavior, and the incorporation of known clinical results for calibration and testing [25]. These and other similar computational methods may help to accelerate the drug development process and stimulate confidence in novel therapies in pre-clinical settings [26,27].

Therefore, we have assembled a computational pipeline capable of taking observed animal model effects of treatments, simulating host immunological and microbial changes, and predicting scaled clinical scores. To display the effectiveness of the pipeline, we use its stochastic simulation and machine learning methods to replicate the displayed efficacy of recent therapeutic advancements, fecal microbiota transplantation, and anti-toxin antibodies, in comparison to standard antibiotics. Further, we use the model to predict the effectiveness of a novel immune-based *C. difficile* treatment, LANCL2 activation to induce immunoregulation and validate the predictions in an animal model of the disease. The novel platform has the potential to accelerate the development of novel immunoregulatory treatments for the infectious and immune-mediated disease.

2. Methods

2.1. Model pipeline

The model pipeline (Fig. 1) uses a previously calibrated and described tissue level model of *C. difficile* infection, which is publically available from the BioModels repository [5]. The fifteen most sensitive parameters from previous analysis were then re-calibrated to fit mouse model data corresponding to treatments that have progressed to the clinical trial stage. This data was found by first identifying treatments for which clinical data was deposited in clinicaltrials.gov or publicly available [9,11,21,28]. Clinical data largely consisted of population level data with a number of adverse effects, recurrent episodes and length of hospital stay being the main parameters. The treatment and associated research group were then searched to find the corresponding preclinical animal testing of the proposed treatment. After the recalibration of the model for each treatment, the model was stochastically simulated using the τ-Leap method for 50 replications on the Condor-Copasi web server [29]. Based on cellular-level sensitivity analysis, six simulation outputs were parsed from each replication and normalized to values between 0.1 and 1.5 for simulation output.

The outputs were then translated to clinical predictions using an ensemble of machine learning methods of neural networks (hidden nodes = 8, err.fct = sse, threshold = 0.005), random forest (mtry = 3–4, ntree = 800–1500), and support vector machines (epsilon = seq(0,1,0.1), cost = $2\hat{}$(2:9)) [30–32]. For known treatments (those with both animal and clinical data), the machine learning algorithms were trained and tested through 10 fold cross validation methods. Briefly, the 50 simulated replicates were randomly assigned a value within the allowable variation in the clinical data for each clinical outcome selected from a normal distribution. The 50 simulated replicates were then divided into 10 groups. Systematically, nine out of the ten groups were selected for each known treatment and used as the training dataset while the remaining group was withheld and used for testing of the predictions. The five best performing training sets, by variation from the testing dataset, were then used for predictions. For predictions, the 50 simulated replicates were assessed by each of the five best performing machine learning models and averaged across the three algorithms. Principal component analysis (PCA) was conducted in R using combined data from six stochastic simulation outputs and the three predicted clinical outcomes. Single parameter knockouts were generated by reverting one parameter change to the 'wild-type control' value.

2.2. Ethics statement

All experimental procedures were approved by the Institutional Animal Care and Use Committee (IACUC) of Virginia Tech and met or exceeded requirements of the Public Health Service/National Institutes of Health and the Animal Welfare Act. C57BL/6J mice were bred and maintained in experimental facilities at Virginia Polytechnic Institute and State University. Mice were euthanized prior to scheduled end point if severe signs of illness, such as a large weight loss, piloerection or a loss of mobility, were present.

2.3. C. difficile *animal model*

This study followed a previously reported model of *Clostridium difficile* infection [5,33,34]. Prior to bacterial challenge, mice were treated with a mixture of antibiotics in drinking water: colistin 850 U/mL (4.2 mg/kg), gentamycin 0.035 mg/mL (3.5 mg/kg), metronidazole 0.215 mg/mL (21.5 mg/kg), and vancomycin 0.045 mg/mL (4.5 mg/kg), followed by an intraperitoneal injection of clindamycin, 32 mg/kg, one day prior to infection. The infectious challenge was with *C. difficile* strain VPI 10463 (ATCC 43255) 10^7 cfu/mouse in Brucella broth via gavage. Mice on NSC61610 treatment received 20 mg/kg/day via gavage in sterile PBS beginning 24 h post-infection.

2.4. Sample processing

Colon samples were washed in BD Cell Recovery Media to remove epithelial cells. The remaining tissue was digested in RPMI containing collagenase and DNase at 37 °C while stirring. Samples were filtered using and centrifuged. Remaining cells were re-suspended and purified in a Percoll gradient. Cells at the Percoll interface were collected and counted.

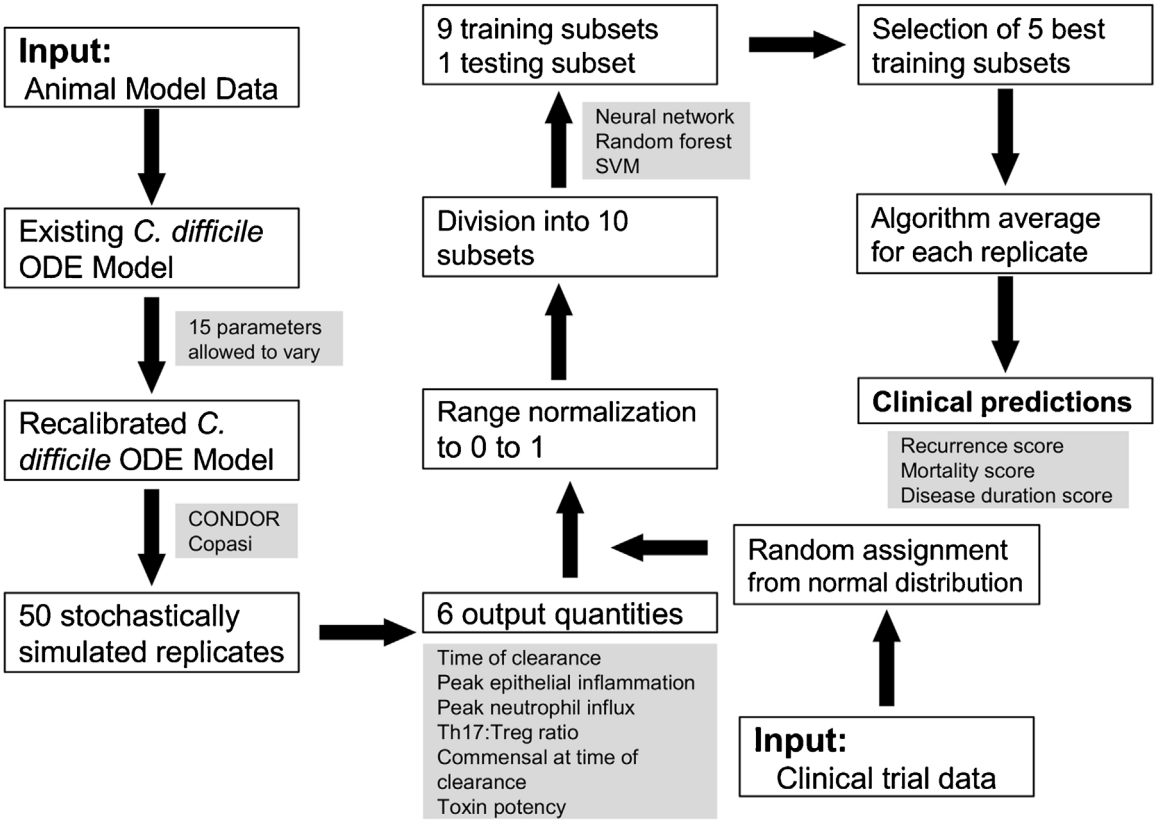

Fig. 1. Schema of the computational pipeline for the translation of animal model data to predicted clinical measures.

2.5. Flow cytometry

Cells were incubated with fluorochrome conjugated antibodies to extracellular markers, anti-CD45 APC-Cy7, anti-CD3 PE-Cy5, anti-CD4 PE-Cy7, anti-CD25 biotin, anti-CD64 PE, anti-CD11b AlexaFluor700, anti-F4/80 PE-Cy5, anti-CD11c FITC, anti-Gr1 PE-Cy7, anti-Ly6c PerCP-Cy5.5, and anti-MHC-II biotin. Samples needing a secondary staining were incubated with Streptavidin-Texas Red. The samples were then fixed and permeabilized. Cells were incubated with antibodies to intracellular markers, anti-FoxP3 FITC, anti-IL-10 APC, anti-RORγT PE, and anti-IL-17 APC. Data was acquired with a BD LSRII flow cytometer and analyzed using FACS Diva software (BD Pharmingen).

2.6. Bacterial Re-isolation

Colonic contents were collected from excised colons. Samples were homogenized in Brucella broth and incubated at 68 °C for one hour. Samples were centrifuged at 10,000 rpm for 30 s and the supernatant was collected. The supernatant was serially diluted (1:10, 1:100, 1:1000) and plated on Oxoid Clostridium difficile agar plates containing *Clostridium difficile* selective supplement. Plates were incubated in anaerobic conditions using a BD EZ anaerobic container system kit for 2 days at 37 °C. Colonies were counted and compared to sample weight for normalization.

2.7. Gene expression

Total RNA was isolated from mouse colonic contents using a Qiagen RNA isolation mini kit. Complementary DNA (cDNA) was generated from each sample using the iScript cDNA synthesis kit. Standards were produced through a polymerase chain reaction on the cDNA with Taq DNA polymerase from Invitrogen. The amplicon was purified using the Mini-Elute PCR purification kit from Qiagen. Expression levels were obtained through quantitative real-time PCR on a Bio-Rad CFX 96 Thermal Cycler using the Bio-Rad SYBR Green Supermix. For analysis, the starting amount of anti-microbial peptide cDNA was compared to that of beta-actin, as a control.

2.8. Statistical analysis

A one-way (genotype) ANOVA was performed to determine significance in the data using a SAS (SAS Institute) general linear model procedure. Differences of $p \leq 0.05$ were considered significant. The number of samples per for each group varied between five and eight. Data is displayed as mean values with error bars representing standard error of the mean and asterisks to indicate statistical significance.

3. Results

3.1. Model development: stochastic simulation displays decreased immune activation and epithelial damage with alternative therapies

Using the previously calibrated ODE model of interactions between *C. difficile*, the host, and commensal microbiota, the effects of four treatments were tested [5]. The host-pathogen-microbiota interaction model describes the interactions between immune cells, epithelial cells, *C. difficile* and commensal microbiota with 23 ODEs containing 49 parameters. Briefly, parameters control the rates of death, proliferation, and activation of the different cell types within the model to capture the immune response, the regrowth of commensal species post-antibiotics, the burden of *C. difficile* and the damage to the epithelium. Sensitivities of each parameter were calculated by a finite difference method of numerical

differentiation. Using sensitivity analysis of the ODE model, 15 sensitive parameters, parameters most likely to affect the outcome of the simulation and most likely to be affected by the proposed treatments, were selected from the complete set of 49. The chosen parameters are all rate constants for mass action kinetics or maximum forward velocities for Hill-type or Michaelis-Menten kinetics. Commensal death and commensal regrowth are parameters controlling the abundance of beneficial commensal bacteria within the model. The presence of certain strains of commensal bacteria has been shown to correspond to accelerated recovery and lower rates of recurrence. Meanwhile, commensal harmful death influences the presence of harmful commensal microbiota, bacteria that promote *C. difficile* expansion. Cdiff growth and Cdiff death control the life cycle and overall burden of *C. difficile*. The parameters, tDC production and eDC production, mediate the polarization of dendritic cells into tolerogenic and effector phenotypes based on their exposure to luminal microbiota. Dendritic cells are strong controllers of whether the immune response to *C. difficile* becomes amplified based on their interaction with CD4+ T cells post-activation. M activation is associated with the production of inflammatory macrophages from infiltrating monocytes, while N activation/migration is associated with the recruitment and activation of neutrophils to the mucosa. Both populations help to eliminate C. difficile from the simulation space but also have the potential for damaging host cells. E damage and E inflame are two parameters that describe the status of epithelial cells and whether they become inflamed, producers of inflammatory mediators to activate the immune response, or damaged, less functional cells that struggle to maintain the epithelial barrier. The final four parameters, Th1 differentiation, Th17 plasticity, Treg differentiation, Th17 differentiation, all control respective parts of the balance and differentiation of CD4+ T cells into Th1, Th17 and iTreg phenotypes. The relative balance between inflammatory and regulatory CD4+ T cells has been strongly associated with improved disease prognosis [5,8].

Based on the treatment specific recalibration, the 15 sensitive parameters were varied within the model to mimic the effects of each individual treatment (Table 1). With a τ-Leap method of stochastic simulation, each treatment was simulated 50 times. From this simulation, large effects were observed on immune activation for the antibody, LANCL2, and fecal microbiome transplantation (FMT) treatments compared to antibiotic treatment. The change in simulated neutrophil influx is shown as a representative quantity of immune activation effects (Fig. 2A–D). As expected, FMT treatment was predicted to have the largest effect on commensal bacteria regrowth while LANCL2 activation displayed lesser but similar beneficial effects (Fig. 2E–H). Anti-toxin antibody treatment did not display major differences compared to standard antibiotic treatment. However, the model predicts that only antibody treatment is capable of significantly decreasing epithelial inflammation during the course of infection (Fig. 2I–L).

3.2. Model simulation: non-antibiotic therapies predicted to have beneficial effects on clinical measures

The abundance of information resulting from the stochastic simulations increases the difficulty of comparing the effectiveness of various treatments. Therefore, we incorporated a machine learning step to accept the simulated time course responses and output lumped scoring parameters similar to clinical measurements from 0 (most beneficial) to 1 (least beneficial). The optimization of the machine learning algorithms occurred in two parts. First, the main parameters (NN: hidden nodes, threshold; RF: mtry, ntree; SVM: epsilon, cost) for each algorithm were scanned using the entire training database to select the best performing parameters by error minimization. Second, with parameters in place, the algorithms were trained using ten-fold cross validation methods to withhold data to avoid sample bias and prevent over-fitting. The prediction of the three algorithms was averaged together for each replicate to provide the final scores for that replicate. The resul-

Table 1
Percent changes of default parameters needed to capture treatment effects.

	Antibiotics	FMT	Antibodies	LANCL2
Commensal Death	75	0	0	0
Cdiff Growth	-20	-5	0	0
Commensal Harmful Death	0	20	0	0
Cdiff Death	0	35	0	0
Commensal Regrowth	0	400	0	20
tDC Production	0	-10	-10	20
eDC Production	0	0	-10	0
M Activation	0	0	-30	-10
N Activation/Migration	0	0	-40	-10
E Damage	0	0	-40	0
E Inflame	0	0	-40	0
Th1 Differentiation	0	0	0	-10
Th17 Plasticity	0	0	0	50
Treg Differentiation	0	0	0	50
Th17 Differentiation	0	0	0	-20

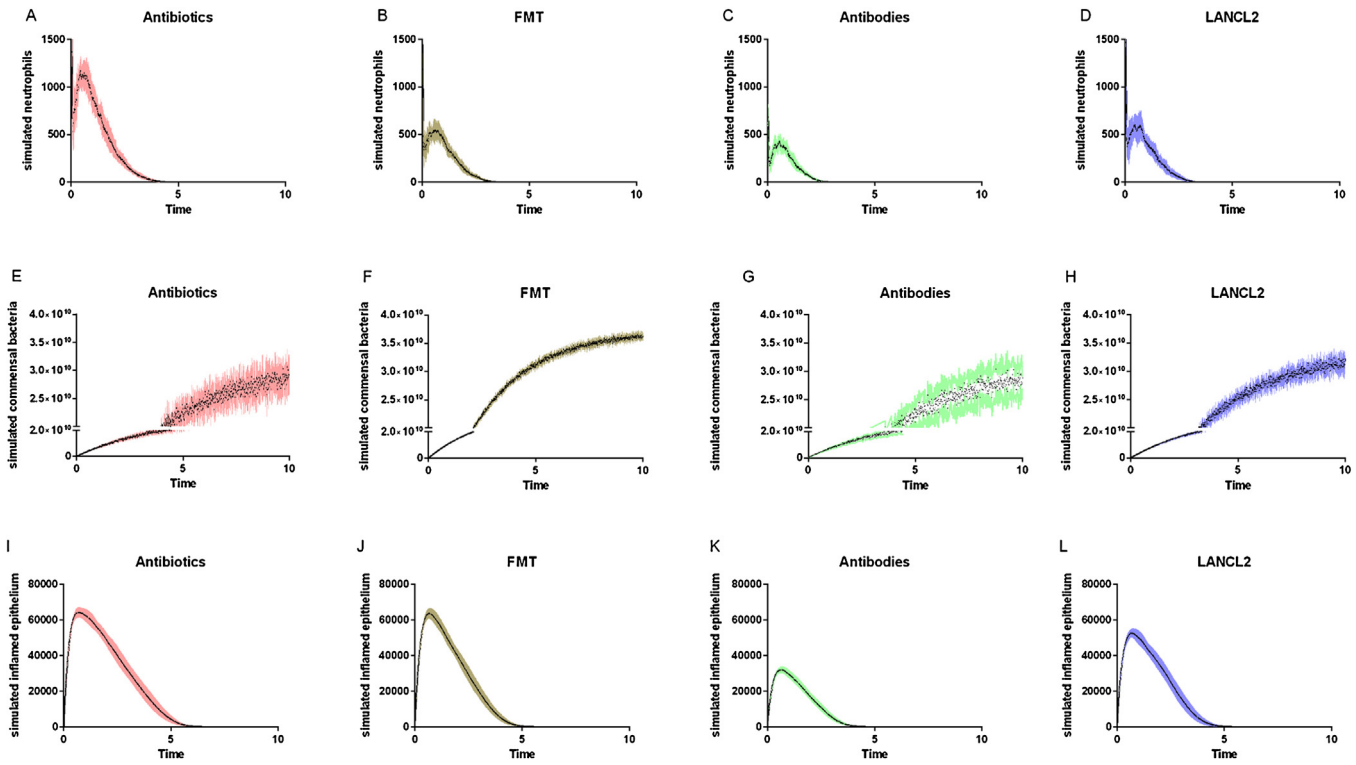

Fig. 2. Stochastic simulation results of *C. difficile* response model. Treatment-calibrated models for antibiotics, fecal microbiome transplantation (FMT), anti-toxin antibodies and LANCL2 activation was stochastically simulated with 50 replicates on CONDOR Copasi. Predicted effects on simulated neutrophils (A–D), commensal bacteria (E-H), and epithelial inflammation (I-L) for each treatment over a ten day simulated time course.

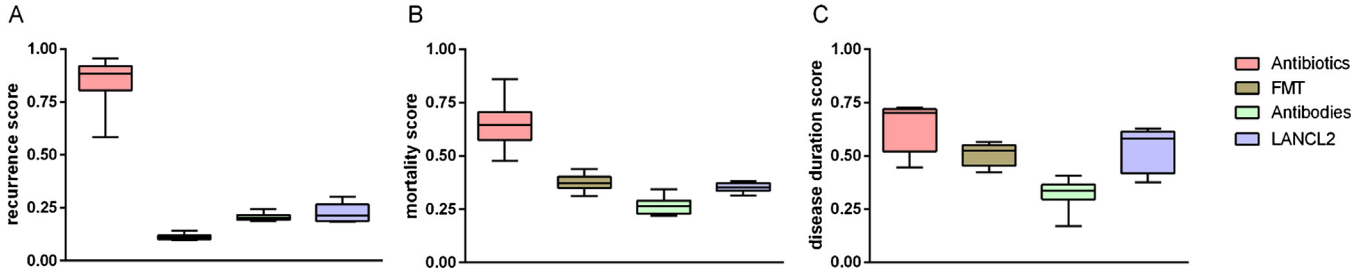

Fig. 3. Comparative *in silico* clinical outcomes across treatments. Machine learning algorithms were used to translate simulation results into clinical scores. Antibiotics, fecal microbiome transplantation (FMT), anti-toxin antibodies and LANCL2 activation were compared. Normalized summary scores were prepared on a range from 0 (most beneficial) to 1 (least beneficial) for recurrence (A), mortality (B) and duration of disease (C).

tant lumped scoring measures, recurrence, mortality, and disease duration, are the three most important conditions related to the effectiveness of *C. difficile* treatment. When comparing the four treatments, antibodies, LANCL2 activation, and FMT were more effective than antibiotics across all three measures (Fig. 3A–C). Additionally, antibiotic therapy resulted in the largest degree of variation between simulated replicates. Notably, anti-toxin antibodies performed best in the disease duration score (Fig. 3C) while FMT was most effective in reducing the likelihood of recurrence (Fig. 3A). Further the pairwise combination of the four treatments suggests that novel antibiotic alternatives have complementary effects (Fig. 4A–C). Across the three predicted clinical outcomes, the three combinations featuring two alternative therapies showed high levels of efficacy while the three groups containing antibiotics displayed worsened scores and higher variability in response. Potentially, the highly efficacious combination of antibodies and FMT, antibodies and LANCL2 activation or LANCL2 activation and FMT could be an ideal option for high risk patients in need of greater treatment potency.

3.3. Model simulation: analysis of dosage and impaired efficacy on predicted clinical outcomes

To assess dosage dependencies and the effects of treatment on patients who may experience reduced benefits, we simulated the computational pipeline at scaled efficiencies for each treatment. The parameter effects of each treatment were adjusted to 10%, 25%, 50%, and 75% of the original calibrated value (100%) for the corresponding treatment. LANCL2 (Fig. 5A–C) and anti-toxin antibody (Fig. 5G–I) treatments profiled similarly with loss of recurrence effects between 50% and 75%, loss of mortality effects between 75% and 100% and scattered to no effects on duration effects down to 10%. Alternatively, FMT (Fig. 5D–F) displayed benefits of treatment on recurrence down to 10%, while effects on mortality and duration were lost around 75% for both. In contrast, the reduction in antibiotic dosage/efficacy (Fig. 5J–K) to 50% resulted in improved recurrence, mortality and duration scores suggesting that lower doses of antibiotics could help to balance beneficial effects of

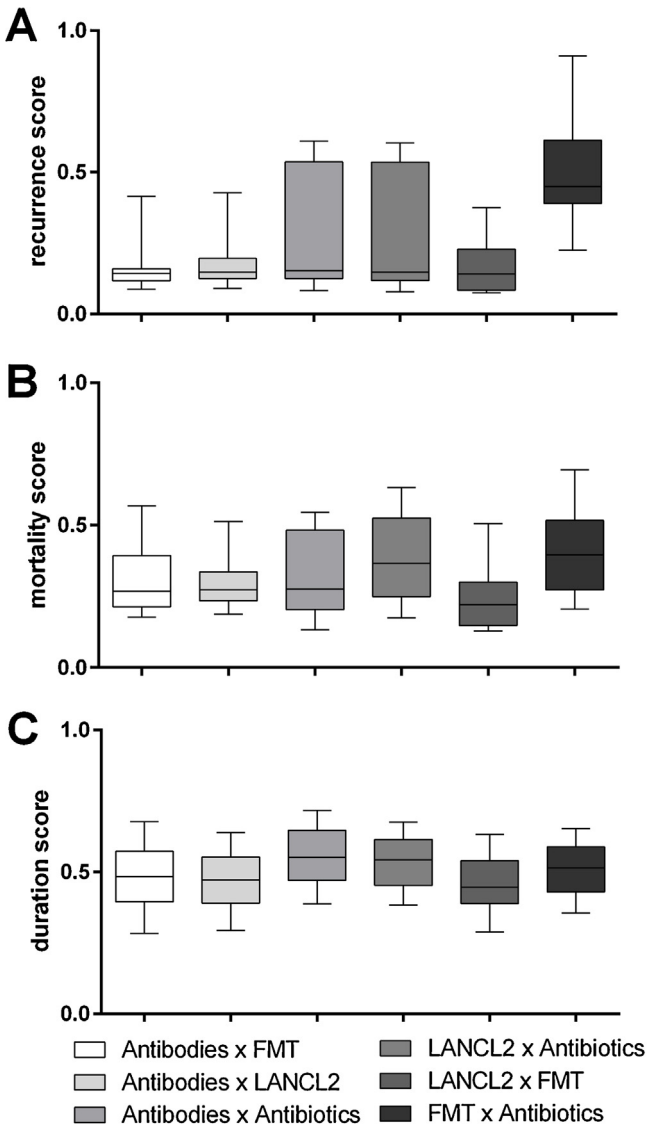

Fig. 4. Combination *in silico* treatments identify cooperativity in antimicrobial alternatives. Treatment effects for each of the four treatments were combined in a pairwise manner. The computational pipeline was used to generate recurrence (A), mortality (B), and duration (C) scores for each of the resultant six groups.

eliminating *C. difficile* with its deleterious effects of inhibiting commensal bacteria regrowth.

3.4. Model analysis: principal component analysis (PCA) enabled assessment of treatment parameter sensitivity

To identify the critical effects promoted by each treatment, we created single parameter knockouts of each of the parameter effects indicated in Table 1. Each knockout then underwent the remaining steps of the pipeline to predict clinical effects. To assess the similarity of each knockout to the original treatment, we used PCA on the six normalized stochastic outputs and the three clinical predictions. Principal components 2 and 3 were utilized as component 1 was a result of largely within group variation. Principal component 2 placed high weight on commensal bacteria, inflamed epithelial cells, mortality, and recurrence. Principal component 3 placed high weight on clearance, T cell ratio, mortality, and recurrence. Removal of the impact of antibiotics on the death of beneficial commensal bacteria significantly improved the disease response in comparison to the control antibiotic treatment while the removal of the effect on *C. difficile* death worsened the response (Fig. 6A). This suggests that while highly specific antibiotics could be an effective therapy, the risk for a resistant strain of *C. difficile* completely negates the efficacy. The effect of fecal microbiome transplantation was largely reliant on the ability to influence commensal regrowth while an inability to induce tolerogenic dendritic cells created more variation in response to treatment (Fig. 6B). Single parameter knockouts within LANCL2 treatment resulted in two noticeable shifts (Fig. 6C). The first was the loss of an effect on commensal regrowth which varied along component 2. The second shift could occur through loss of either tolerogenic dendritic cell production or T cell plasticity and resulted in a shift along component 3. Notably, the second shift closely associated with antibiotic treatment when compared while control LANCL2 treatment associated with fecal microbiome transplantation (Fig. 6D).

The single parameter effects were confirmed by directly examining the duration, mortality and recurrence scores for each parameter knockout. The antibiotic treatment lacking effect on beneficial commensal death had improved mortality and recurrence (Fig. 7B–C). The fecal microbiome transplantation lacking commensal regrowth had worsened recurrence (Fig. 7F). Similarly, the LANCL2 treatment lacking commensal regrowth had worsened recurrence (Fig. 7I). Meanwhile, T cell plasticity and tolerogenic dendritic cell effect knockouts had slightly worsened responses across all three scores (Fig. 7G–I).

3.5. Model analysis: T cell ratio correlates with improved treatment and disease responses

To observe if the dependency on T cell responses was consistent across treatments, we assessed the correlation between clinical outcome scores and Treg to Th17 ratio (Fig. 8A–C). A noticeable downward trend was observed with high Treg to Th17 ratios correlating with lower disease duration, mortality and recurrence scores. Notably, the non-responders (virtual patients with scores above 0.5 in one of the three clinical outcomes) had consistently low T cell ratios. To observe if this trend persisted within only LANCL2 treatment, we separate non-responders from responders. The non-responders to LANCL2 treatment had on average a 50% lower Treg to Th17 ratio compared to responders (Fig. 8E). A smaller but similar trend was observed within the quantity of commensal bacteria (Fig. 8D); however, no trend was observable in *C. difficile* clearance between LANCL2 responders and non-responders (Fig. 8F). Sensitivity analysis of the full set of T cell parameters displays potent effects of Th17 migration, Th17:Treg plasticity and Treg death on epithelial death, C. difficile burden, the regrowth of commensal bacteria, and neutrophil activation (Fig. 8G–J). This confirmation of the importance of a Treg to Th17 ratio further validates the potential of T cell targeted therapies in *C. difficile* infection.

3.6. Experimental validation: loss of LANCL2 in a mouse model of C. difficile infection increases disease severity and colonic inflammation

To assess the validity of LANCL2 as an important molecule in the immune response to *C. difficile*, we infected both wild-type mice and mice deficient in LANCL2 (LANCL2-/-). The loss of LANCL2 accelerated weight loss compared to wild type mice early in infection with significant differences appearing at days 2 and 3 post-infection (Fig. 9A). Meanwhile, persistent increases in disease activity index were observed throughout the time course (Fig. 9B), while little to no differences in re-isolation of *C. difficile* were observed until day 8 post-infection (Fig. 9C). In agreement with disease activity scores, higher percentages of neutrophils and Th17 cells were observed in the colons of infected LANCL2-/- mice compared to infected WT (Fig. 9D-E).

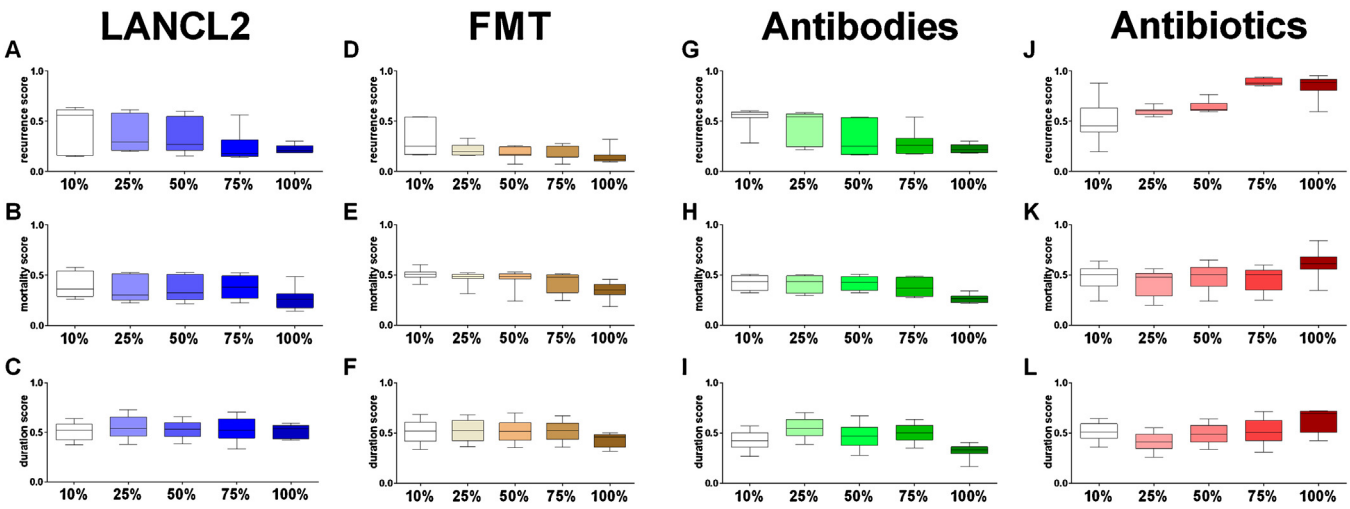

Fig. 5. Dosage effects of treatments on recurrence, mortality and duration. Treatment effects for each of the four treatments were scaled down to 10%, 25%, 50% and 75% of their full parameter values to assess the effects of dosage and impaired efficacy on the overall treatment response. The computational pipeline was used to generate recurrence, mortality, and duration scores, respectively, for each of LANCL2 activation (A-C), FMT (D–F), anti-toxin antibodies (G–I), and antibiotics (J–L) the resultant six groups.

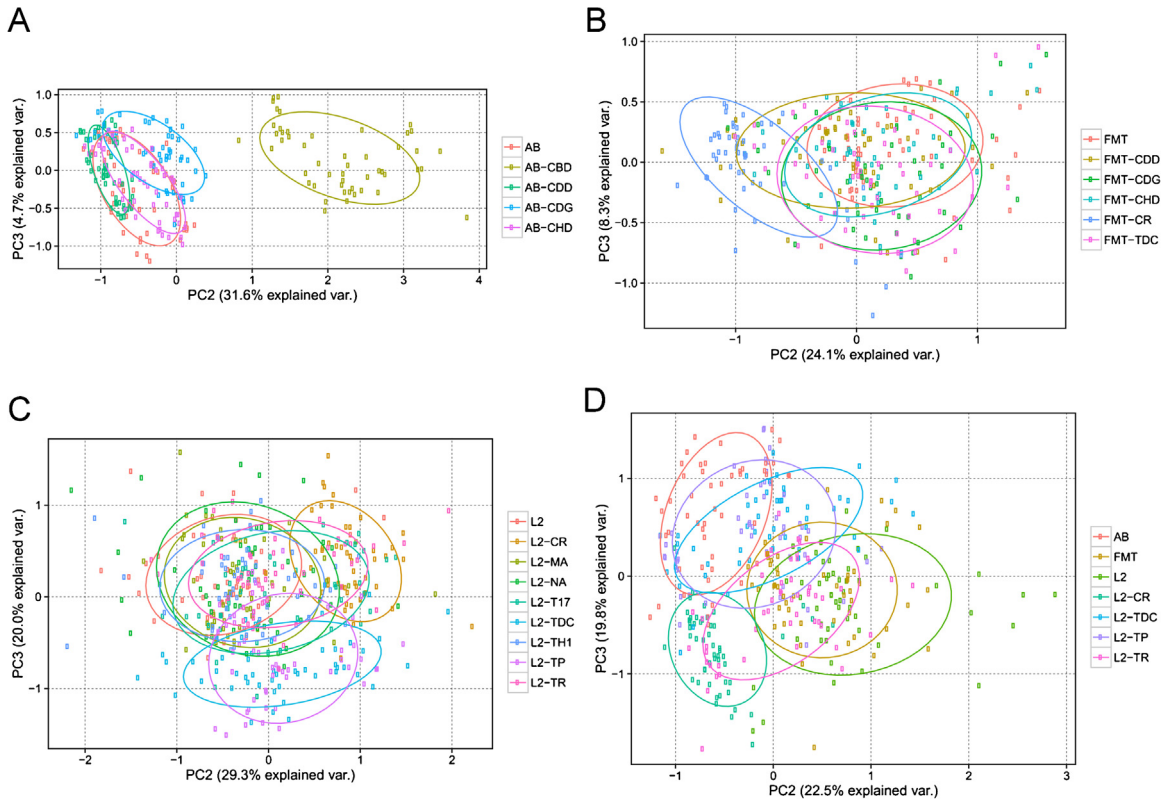

Fig. 6. Principal component analysis of *C. difficile* treatments. Based on the six stochastic simulation outputs (time of clearance, peak epithelial inflammation, peak neutrophil influx, Th17:Treg ratio, commensal at the time of clearance and toxin potency) and three *in silico* clinical scores (recurrence, mortality, and duration), treatments were compared using principal component analysis. Single parameter knockouts for antibiotics (A), fecal microbiome transplantation (B), LANCL2 activation (C) are displayed. Knockout abbreviations: beneficial commensal death (*CBD*), C. difficile death (*CDD*), C. difficile growth (*CDG*), harmful commensal death (*CHD*), commensal regrowth (*CR*), macrophage activation (*MA*), neutrophil activation (*NA*), Th17 differentiation (*T17*), tolerogenic dendritic cell activation (*TDC*), Th1 differentiation (*TH1*), T cell plasticity (*TP*), regulatory T cell differentiation (*TR*). Comparison between LANCL2 single parameter knockouts, antibiotics and fecal microbiome transplantation (D).

3.7. Experimental validation: LANCL2 ligand NSC61610 administration lessens clinical signs of disease and cellular markers of inflammation

To determining the viability of LANCL2 activation and subsequent immunoregulation as a *C. difficile* therapeutic option, C57BL/6 wild type mice were infected with *C. difficile* strain VPI10463 and a subset of infected mice was given 20 mg/kg NSC61610 by gavage daily. Mice treated with NSC61610 also experienced significantly less weight loss, with a 10% reduction in maximum percent loss: 8% for the NSC61610 treated the group to 18% for the untreated infected group (Fig. 10A). Mice treated with NSC61610 exhibited a later onset of disease, displaying first symptoms one day later than the untreated infected cohort (Fig. 10B).

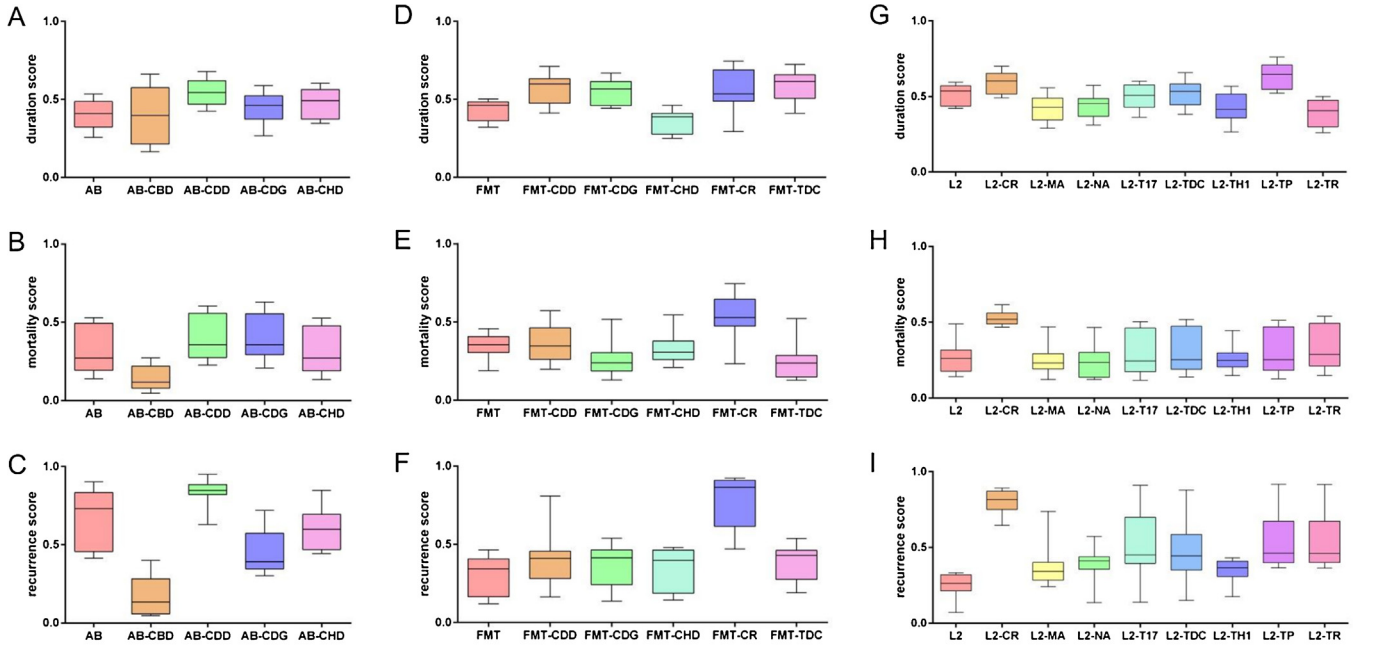

Fig. 7. Single parameter knockout effects on clinical outcome scores. Single parameter knockout effects for antibiotics (A–C), fecal microbiome transplantation (D–F), LANCL2 activation (G–I) are displayed. Knockout abbreviations: beneficial commensal death (*CBD*), C. difficile death (*CDD*), C. difficile growth (*CDG*), harmful commensal death (*CHD*), commensal regrowth (*CR*), macrophage activation (*MA*), neutrophil activation (*NA*), Th17 differentiation (*T17*), tolerogenic dendritic cell activation (*TDC*), Th1 differentiation (*TH1*), T cell plasticity (*TP*), regulatory T cell differentiation (*TR*).

NSC61610-treated mice experienced only mildly loose stools and no changes in activity, compared to the soiled perianal area and reduced activity levels present in the untreated infected group at peak disease on the fourth day post-infection. Additionally, the untreated infected cohort experienced 60% survival, compared to 100% survival in the treated infected group (Fig. 10C).

Colons and colonic contents were collected on day 8 post-infection. Colonic content samples were homogenized, plated, and incubated for 48 h in an anaerobic environment. Mice treated with NSC61610 displayed no significant difference in the amounts of *C. difficile* than their untreated infected counterparts on day 8 post-infection (Fig. 10D). Portions of colons were fixed and stained with hematoxylin and eosin, prior to grading under microscopic examination. Mice treated with NSC61610 exhibited significantly less leukocytic infiltration, mucosal thickness, and epithelial erosion, showing only mild signs of disease compared to the untreated infected group (Fig. 10E-G). Remaining portions were processed for immunophenotyping by flow cytometry. The NSC61610 demonstrated a large reduction in neutrophils compared to the untreated infected group (Fig. 10H). The NSC61610 group also displayed a significant reduction in the Th17 CD4+ T cell population compared to the untreated infected group (Fig. 10I). Very little variation between the uninfected control group and the NSC61610 group was observed. No differences were observed within macrophage populations between the infected groups. The NSC61610 group also displayed a slight increase in Treg cells on day 8 post-infection (Fig. 10J).

4. Discussion

We have developed an *in silico* clinical trial pipeline for evaluating the efficacy of innovative *C. difficile* treatments. Simulation results, such as these, can be a valuable evaluation method to be used to prioritize therapeutic modalities between the conclusion of nonclinical testing and the beginning of Phase 2 clinical trials. As an alternative to animal models and to guide traditional human clinical trials, *in silico* clinical trials may help to accelerate promising therapeutic candidates reducing the time and cost needed to progress a treatment to practice. In the initial test case, which includes anti-toxin antibodies, LANCL2 activation, fecal microbiome transplantation and antibiotics, the pipeline predicts that the three treatments in development would all be expected to outperform the current conventional therapy, antibiotics. These differences are apparent both in immunological measures as well as predicted effects on clinical measures such as recurrence, mortality, and duration. The ability of alternative therapies to combat gastroenteric pathogens, such as *C. difficile*, lends support that the decreased use of antibiotics and promotion of antibiotic stewardship is not only important, but is also currently possible. Further development of the described pipeline may allow for the creation of a precision medicine tool based on advanced machine learning algorithms that is capable of monitoring disease progression, recurrence, and response to treatment through fecal and blood measurements, to inform the best treatment strategies on a patient-by-patient basis. Essentially, the in silico patients would become avatars for testing personalized medicine treatments computationally before implementing in the clinic.

Iteratively combining computational modeling in concert with experimental validation and biological knowledge in a systems biology cycle can greatly aid in the understanding of the disease and the development of novel therapies [35–37]. The computational methods embedded in our *in silico* pipeline included equation based modeling and machine learning algorithms, are two of the many methods capable of elucidating network dynamics and behavior patterns not evident through traditional means. In particular, we have previously used a mechanistic ODE model of host responses to *C. difficile* to generate non-intuitive hypotheses [5]. In this study, we employed the mechanistic ODE model for the generation of stochastically varied replicates in different treatments, displaying the adaptability of computational models to the desired purpose. As used here, supervised machine learning is a valuable method for the expansion of previously acquired data into new unexplored

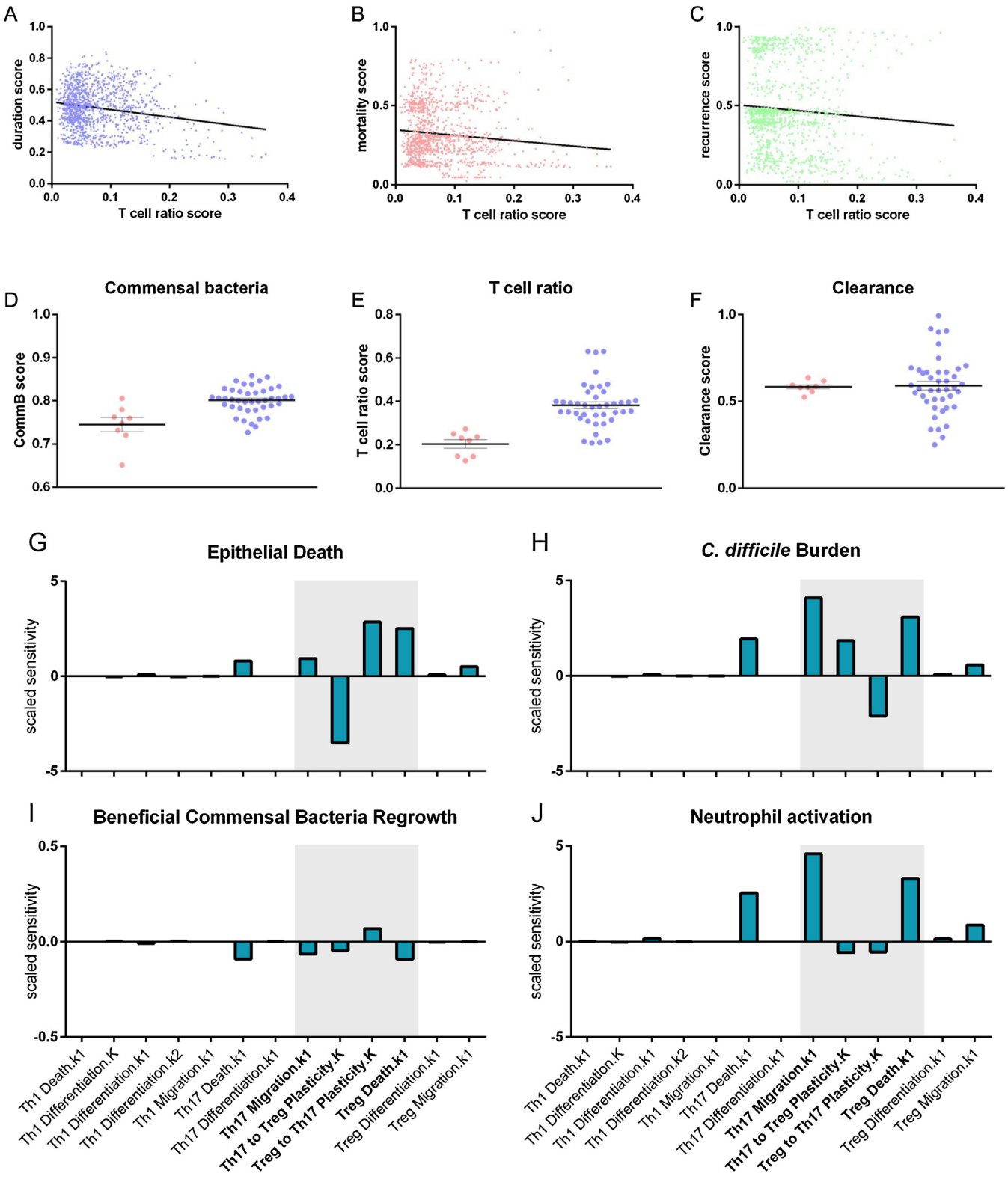

Fig. 8. Correlation of T cell ratio with disease response. Negative correlation exist between Treg to Th17 ratio and disease duration (A), mortality (B), and recurrence (C) scores. For LANCL2 treatment, virtual patients who responded to treatment (duration, mortality, and recurrence scores all below 0.5) were separated from ones that did not. LANCL2 responders had higher commensal bacteria scores (D) and Treg to Th17 ratios (E) with no observable difference in clearance (F). Sensitivity analysis of T cell associated parameters on epithelial cell death (G), C. difficile burden (H), beneficial commensal bacteria regrowth (I), and neutrophil activation (J).

areas [38]. The combination of data-driven and mechanistic modeling can help to ensure that both known biological mechanisms are retained and unknown quantities are not disregarded, without compromising the predictive capability of the system.

Each machine learning algorithm used in this study has comparative advantages to the other two. Neural networks is the best performing with high levels of noise, support vector machines identifies global minima rather than local minima, and random

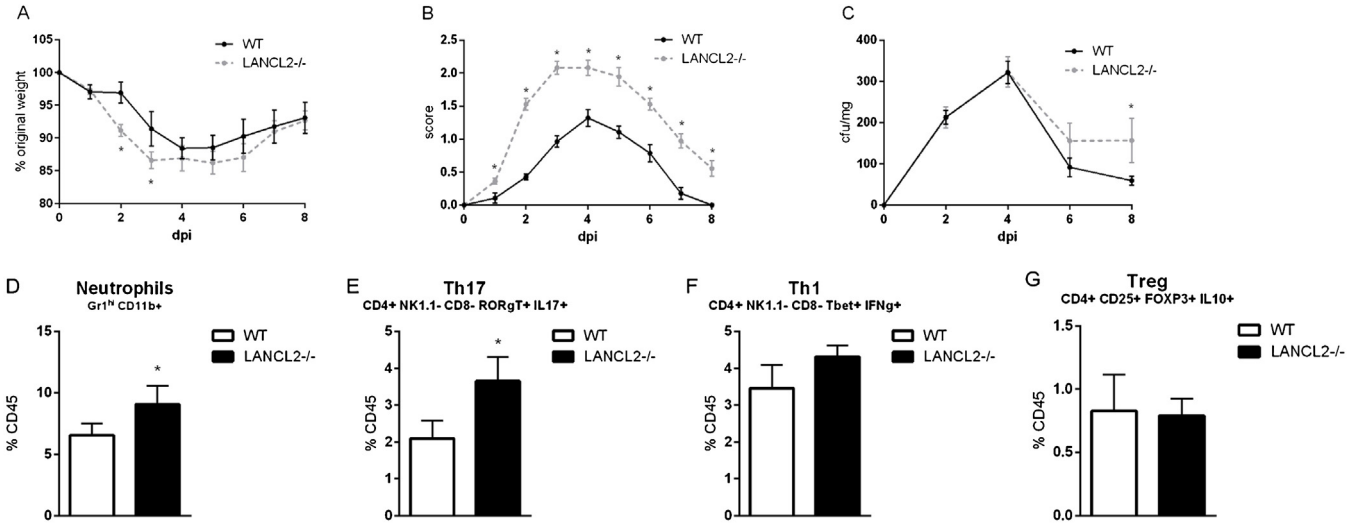

Fig. 9. LANCL2 deficiency increases disease severity. Weight loss (A), disease activity index (B), and *C. difficile* re-isolation (C) in wild-type and LANCL2-/- mice across eight days post-infection. Neutrophils (D), Th17 (E), Th1 (F), and Treg (G) presented as percentage of CD45+ cells within colonic lamina propria at day 8 post-infection. Asterisks (*) mark statistically significant ($p \leq 0.05$) differences between genotypes (n = 8).

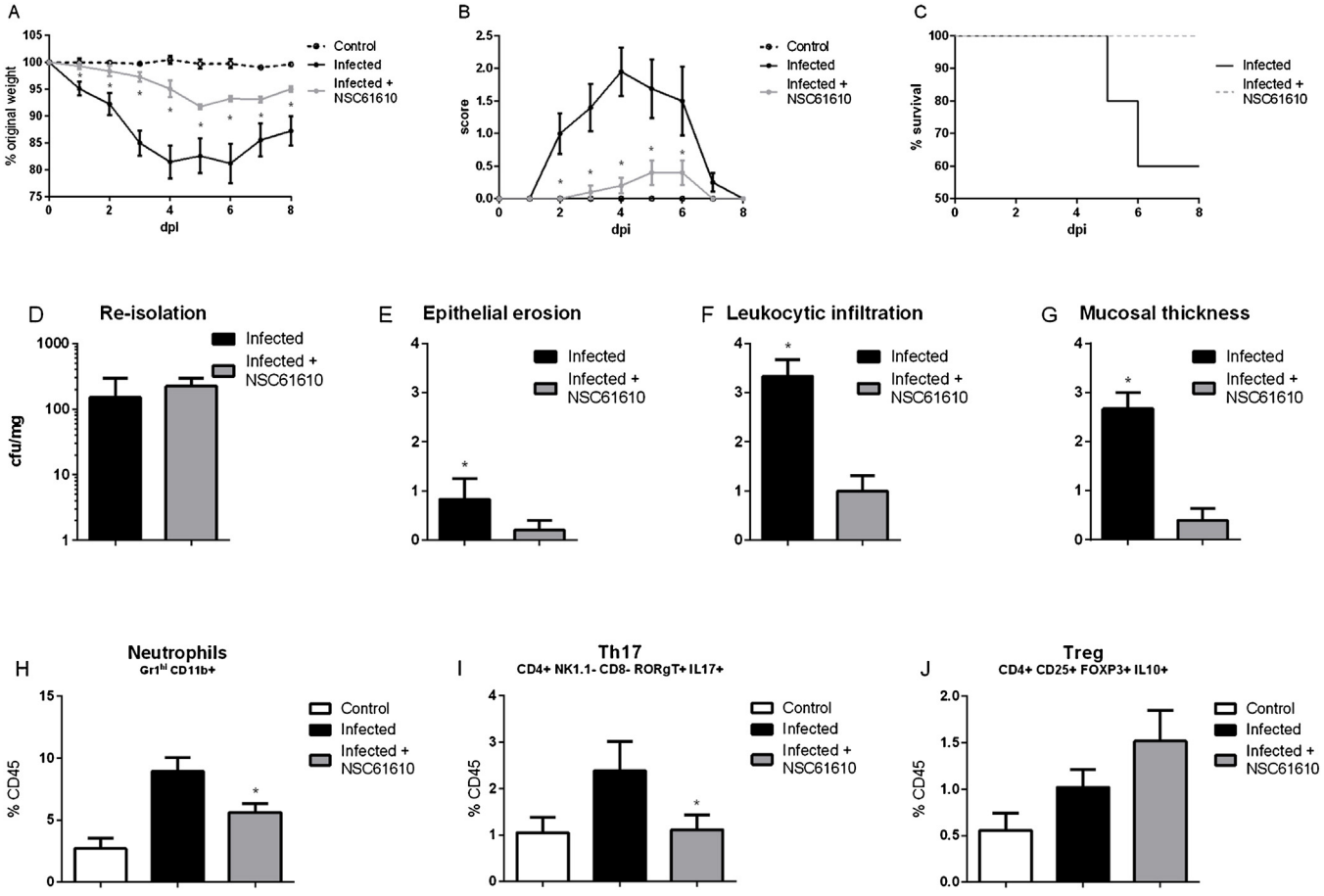

Fig. 10. NSC61610 administration decreases disease severity. Weight loss (A), disease activity index (B), and mortality (C) in wild-type mice untreated and NSC61610 (20 mg/kg/day) treated across eight days post-infection. *C. difficile* reisolation from colonic content on day 8 post-infection (D). Histopathological scores, in epithelial erosion (E), leukocytic infiltration (F), and mucosal thickness (G) of colonic sections eight days post-infection. Neutrophils (H), Th17 (I), and Treg (J) presented as a percentage of CD45+ cells within colonic lamina propria at day 8 post-infection. Asterisks (*) mark statistically significant ($p \leq 0.05$) differences between treated and non-treated groups (n = 8).

forest is robust against over-fitting and relatively insensitive to input parameter settings [39]. The performance of the individual machine learning algorithms was improved through utilization of the three methods as an averaged ensemble rather than individual predictions. Individually, the neural network algorithm provided the lowest error, particularly within the recurrence and mortality

measures. However, during predictions it was the most likely to predict a random shift in one of the three outcome measures. For example, a replicate with low predicted recurrence and duration would also have a very high mortality score. While this is possible biologically, it still brought into question the feasibility of only using neural networks as the main predictor. In contrast, random forest and support vector machines provided very similar predictions to each other across all three categories. The two algorithms, however, tended to be more conservative in testing and prediction phases with a tendency to not capture the full range of scores on both the low and high ends of the spectrum. Therefore, the combination of methods allowed for reduced impact of random score spikes while retaining the capability to identify non- and high-responding populations.

The presented pipeline does have a few differences from other in silico clinical trials and other general limitations in its current version. Rather than generating virtual patients from a seed population of actual patients, our pipeline generates replicates through stochastic simulation of the model. This eliminates any bias present in an initial seed population and allows for broader and more complete coverage of the parameter and response space. However, it also reduces the grounding of the pipeline and virtual patients in real data. Potentially, combining the two methods could help alleviate concerns on either side, thereby removing seed population bias while retaining stochasticity and the biological frameworks providing by patient data. Secondly, the pipeline was generated with sparse human data available from public repositories. The identification of correlations by machine learning provides a strong translation of any murine data used, but for usage within clinical practice a more robust patient dataset containing immunological, host transcriptomics and proteomics, microbial metagenomics, metabolic analyses, and nutritional measurements would be needed.

Aside from the improved efficacy, in terms of lesser probabilities of adverse effects and recurrence events, of the alternatives to the use of antibiotics, the computational simulations and analyses also provided new mechanistic insights. Firstly, the recalibration of the ODE model gave an initial assessment of the network changes induced by each treatment. Based on this assessment, the four treatments clustered in clear microbial effect (antibiotics and FMT) and host effect (antibodies and LANCL2) treatments or as activation (FMT and LANCL2) and inhibition (antibiotics and antibodies) dominant effects. However, post-simulation, the PCA revealed that strong associations existed between the FMT and LANCL2 groups. Unsurprisingly, these two treatments were predicted to have the largest effect on preserving and re-growing the commensal microbiome. Single parameter knockout simulations confirmed this association with loss of commensal regrowth is greatly impacting the recurrence score benefits of each treatment.

It would be tempting to question the fundamental approach of alternative modalities to antimicrobial treatment by suggesting that as opposed to antimicrobials these treatments are not eliminating the original source of the problem. It could even be suggested that non-antimicrobial therapeutics for CDI would require chronic administration. However, this notion of potentially needing chronic treatment is countered by data from Gerding et al., demonstrating that after treatment, non-toxigenic *C. difficile* disappears quite rapidly. The lack of toxin-mediated damage allows the luminal epithelium to recover and the gut microbiome to diversify in a natural process that outcompetes *C. difficile* growth [9]. This data demonstrates that the amount of *C. difficile* becomes marginal over a time of 4–6 weeks, suggesting that the microbiome has begun to diversify and interfere with *C. difficile* colonization. Furthermore, Goldberg et al. also demonstrate that some people are carriers of non-toxigenic *C. difficile* at low levels and that does not trigger any pathogenicity or need for a chronic treatment [40]. It is well established that the microbiome has the capacity to quickly diversify [41] and help overcome infections [42]. In contrast, the use of antibiotics harshly disrupts the microbiome, thereby opening the door to opportunistic infections, and could create antibiotic-resistant bacteria. Antimicrobial alternatives explored here are in line with the White House plan to combat antibiotic-resistant bacteria, provide microbiome preservation and antibiotic stewardship, and develop new antibiotic-free therapeutics for treating CDI [43]. Moreover, *C. difficile* has not become resistant to current antibiotics suggesting that it is relatively stable and unlikely to evolve into producing new toxins as one reviewer suggested. Finally, Buffie et al. [44] demonstrates that normal microflora converts by-products, such as bile salts, that help fight against pathogenic *C. difficile*. Thus, investigating the feasibility of our proposed new paradigm is supported by multiple studies.

The mouse data presented demonstrates that a reduction in disease severity is possible without a reduction in *C. difficile* burden, thereby suggesting that the severity of disease and the persistence and burden of *C. difficile* are not directly correlated. In other words, colonic inflammation and disease can be caused by the presence of CDI, but the presence or expansion of *C. difficile* within the colon does not need to predicate disease. Many of the symptoms of *C. difficile* associated disease (CDAD) are rather the result of over-exuberant inflammatory responses of the host immune system [45]. For example, *C. difficile* toxin A, TcdA, is responsible for the initiation of disease through interaction with epithelial cells causing a disruption in barrier integrity [46]. Potentially, the loss of commensal species following antibiotic treatment could enhance the susceptibility of epithelial cells through a reduction of tolerance-mediated barrier maintenance. Indeed, in a non-disease state, the administration of antibiotics reduces the expression of tight junctions and ion exchangers in the intestinal epithelium [47]. Pharmacologic induction of tolerance through LANCL2 activation could mitigate this barrier weakening step.

Further, even after epithelial barrier disruption, many inflammatory responses are a result of the second *C. difficile* toxin, TcdB, and formerly commensal species rather than the bacterium itself [48,49]. A decreased responsiveness to TcdB may partially ameliorate the severe inflammation related to CDAD as seen through the effectiveness of anti-toxin B antibodies in initial trials and their predicted effectiveness in our *in silico* pipeline [21]. Combined with the TcdB-driven inflammation, the translocation of commensal microbial species may drive further immunoinflammatory reactivity to luminal bacteria, which exacerbates the situation, as the removal of these non-harmful species is not necessary beyond containment of the ones that infiltrated upon disruption of barrier function [50]. Taken together, maintaining tolerogenic responses and barrier function are more important in the prevention of disease and recurrence rather than the clearance of *C. difficile*.

CDI is also strongly associated with changes in the intestinal microbiome [18]. The preservation and restoration of the microbiome through decreased antimicrobial usage and fecal transplantation has become acknowledged as a potential treatment for CDI [11]. Recently, it has been shown that specific functional families of bacteria, such as those responsible for the metabolism of secondary bile acids, butyrogenic bacteria and non-toxigenic *C. difficile*, confer resistance to CDAD [9,51,52]. Further, *C. difficile* can be identified in small quantities within the microbiome of many healthy individuals [53]. This suggests that the ability of *C. difficile* to thrive within the colonic environment is significantly hindered by the presence of intact gut flora, possibly through a competitive inhibition based on substrate availability. An elevated *C. difficile* population that is present during CDI, may be able to be attenuated and slowly decreased

solely by the regrowth of commensal bacteria [51]. Consequently, the immune-mediated clearance of *C. difficile*, resulting from the large degree of pro-inflammatory responses, may be unnecessary comparatively to the inhibitory effect of native commensal bacteria.

The presented *in silico* pipeline for the translation of mechanistic animal model data to predicted clinical outcomes can be an important resource for the development of CDI treatments and an adaptable method for the evaluation of treatments in other diseases. As such, the pipeline aided in the prediction of efficacy of LANCL2 based therapies in CDAD. These predictions are in line with the preliminary animal model results of NSC61610 treatments, through reduction of disease severity and associated inflammation. Therefore, a therapeutic intervention promoting regulatory responses during CDI can be effective in lessening disease severity without causing detrimental effects on the ability to reduce *C. difficile* load.

References

[1] Lessa FC, Winston LG, McDonald LC. Burden of Clostridium difficile infection in the United States. N Engl J Med 2015;372:2369–70.
[2] Cornely OA, Miller MA, Louie TJ, Crook DW, Gorbach SL. Treatment of first recurrence of Clostridium difficile infection: fidaxomicin versus vancomycin. Clin Infect Dis 2012;55(Suppl. 2):S154–161.
[3] Pepin J, Alary ME, Valiquette L, Raiche E, Ruel J, Fulop K, et al. Increasing risk of relapse after treatment of Clostridium difficile colitis in Quebec, Canada. Clin Infect Dis 2005;40:1591–7.
[4] Vindigni SM, Surawicz CM. C. difficile infection: changing epidemiology and management paradigms. Clin Transl Gastroenterol 2015;6:e99.
[5] Leber A, Viladomiu M, Hontecillas R, Abedi V, Philipson C, Hoops S, et al. Systems modeling of interactions between mucosal immunity and the gut microbiome during Clostridium difficile infection. PLoS One 2015;10:e0134849.
[6] Debast SB, Bauer MP, Kuijper EJ. European Society of Clinical Microbiology and Infectious Diseases: update of the treatment guidance document for Clostridium difficile infection. Clin Microbiol Infect 2014;20(Suppl. 2):1–26.
[7] Surawicz CM, Brandt LJ, Binion DG, Ananthakrishnan AN, Curry SR, Gilligan PH, et al. Guidelines for diagnosis, treatment, and prevention of Clostridium difficile infections. Am J Gastroenterol 2013;108:478–98, quiz 499.
[8] El Feghaly RE, Stauber JL, Deych E, Gonzalez C, Tarr PI, Haslam DB. Markers of intestinal inflammation, not bacterial burden, correlate with clinical outcomes in Clostridium difficile infection. Clin Infect Dis 2013;56:1713–21.
[9] Gerding DN, Meyer T, Lee C, Cohen SH, Murthy UK, Poirier A, et al. Administration of spores of nontoxigenic Clostridium difficile strain M3 for prevention of recurrent C. difficile infection: a randomized clinical trial. JAMA 2015;313:1719–27.
[10] Leav BA, Blair B, Leney M, Knauber M, Reilly C, Lowy I, et al. Serum anti-toxin B antibody correlates with protection from recurrent Clostridium difficile infection (CDI). Vaccine 2010;28:965–9.
[11] van Nood E, Vrieze A, Nieuwdorp M, Fuentes S, Zoetendal EG, de Vos WM, et al. Duodenal infusion of donor feces for recurrent Clostridium difficile. N Engl J Med 2013;368:407–15.
[12] Sturla L, Fresia C, Guida L, Bruzzone S, Scarfi S, Usai C, et al. LANCL2 is necessary for abscisic acid binding and signaling in human granulocytes and in rat insulinoma cells. J Biol Chem 2009;284:28045–57.
[13] Bruzzone S, Ameri P, Briatore L, Mannino E, Basile G, Andraghetti G, et al. The plant hormone abscisic acid increases in human plasma after hyperglycemia and stimulates glucose consumption by adipocytes and myoblasts. FASEB J 2012;26:1251–60.
[14] Zeng M, van der Donk WA, Chen J. Lanthionine synthetase C-like protein 2 (LanCL2) is a novel regulator of Akt. Mol Biol Cell 2014;25:3954–61.
[15] Lu P, Hontecillas R, Horne WT, Carbo A, Viladomiu M, Pedragosa M, et al. Computational modeling-based discovery of novel classes of anti-inflammatory drugs that target lanthionine synthetase C-like protein 2. PLoS One 2012;7:e34643.
[16] Carbo A, Gandour RD, Hontecillas R, Philipson N, Uren A, Bassaganya-Riera J. An N,N-bis(benzimidazolylpicolinoyl)piperazine (BT-11): a novel lanthionine synthetase C-like 2-based therapeutic for inflammatory bowel disease. J Med Chem 2016;59:10113–26.
[17] Bissel P, Boes K, Hinckley J, Jortner BS, Magnin-Bissel G, Werre SR, et al. Exploratory studies with BT-11: a proposed orally active therapeutic for Crohn's disease. Int J Toxicol 2016;35:521–9.
[18] Lewis BB, Buffie CG, Carter RA, Leiner I, Toussaint NC, Miller LC, et al. Loss of microbiota-mediated colonization resistance to Clostridium difficile infection with oral vancomycin compared with metronidazole. J Infect Dis 2015;212:1656–65.
[19] Hutton ML, Mackin KE, Chakravorty A, Lyras D. Small animal models for the study of Clostridium difficile disease pathogenesis. FEMS Microbiol Lett 2014;352:140–9.
[20] Babcock GJ, Broering TJ, Hernandez HJ, Mandell RB, Donahue K, Boatright N, et al. Human monoclonal antibodies directed against toxins A and B prevent Clostridium difficile-induced mortality in hamsters. Infect Immun 2006;74:6339–47.
[21] Lowy I, Molrine DC, Leav BA, Blair BM, Baxter R, Gerding DN, et al. Treatment with monoclonal antibodies against Clostridium difficile toxins. N Engl J Med 2010;362:197–205.
[22] Brown D, Namas RA, Almahmoud K, Zaaqoq A, Sarkar J, Barclay DA, et al. Trauma in silico: individual-specific mathematical models and virtual clinical populations. Sci Transl Med 2015;7, 285ra261.
[23] Jeena PM, Bishai WR, Pasipanodya JG, Gumbo T. In silico children and the glass mouse model: clinical trial simulations to identify and individualize optimal isoniazid doses in children with tuberculosis. Antimicrob Agents Chemother 2011;55:539–45.
[24] Kovatchev BP, Breton M, Man CD, Cobelli C. In silico preclinical trials: a proof of concept in closed-loop control of type 1 diabetes. J Diabetes Sci Technol 2009;3:44–55.
[25] Abedi V, Lu P, Hontecillas R, Verma M, Vess G, Philipson C, et al. Phase III placebo-Controlled, randomized clinical trial with synthetic crohn's disease patients to evaluate treatment response. In: Arabnia HRaT QN, editor. Emerging Trends in Applications and Infrastructure in Computational Biology, Bioinformatics and Systems Biology. Cambridge, MA: Elsevier; 2015. p. 411–25.
[26] Leber A, Hontecillas R, Tubau-Juni N, Bassaganya-Riera J. Translating nutritional immunology into drug development for inflammatory bowel disease. Curr Opin Gastroenterol 2016;32:443–9.
[27] Verma M, Hontecillas R, Abedi V, Leber A, Tubau-Juni N, Philipson C, et al. Modeling-enabled systems nutritional immunology. Front Nutr 2016;3:5.
[28] Louie TJ, Miller MA, Mullane KM, Weiss K, Lentnek A, Golan Y, et al. Fidaxomicin versus vancomycin for Clostridium difficile infection. N Engl J Med 2011;364:422–31.
[29] Kent E, Hoops S, Mendes P. Condor-COPASI: high-throughput computing for biochemical networks. BMC Syst Biol 2012;6:91.
[30] Hearst MA. Support vector machines. IEEE Intell Syst Appl 1998;13:18–21.
[31] Lagaris IE, Likas A, Fotiadis DI. Artificial neural networks for solving ordinary and partial differential equations. IEEE Trans Neural Netw 1998;9:987–1000.
[32] Liaw A, Wiener M. Classification and regression by randomForest. R news 2.3; 2002. p. 18–22.
[33] Chen X, Katchar K, Goldsmith JD, Nanthakumar N, Cheknis A, Gerding DN, et al. A mouse model of Clostridium difficile–associated disease. Gastroenterology 2008;135:1984–92.
[34] Viladomiu M, Hontecillas R, Pedragosa M, Carbo A, Hoops S, Michalak P, et al. Modeling the role of peroxisome proliferator-activated receptor gamma and microRNA-146 in mucosal immune responses to Clostridium difficile. PLoS One 2012;7:e47525.
[35] Shen B, Ma J, Wang J. Biomedical informatics and computational biology for high-throughput data analysis. Sci World J 2014;2014:398181.
[36] Leung EL, Cao ZW, Jiang ZH, Zhou H, Liu L. Network-based drug discovery by integrating systems biology and computational technologies. Brief Bioinform 2013;14:491–505.
[37] Kitano H. Computational systems biology. Nature 2002;420:206–10.
[38] Jensen LJ, Bateman A. The rise and fall of supervised machine learning techniques. Bioinformatics 2011;27:3331–2.
[39] Lu P, Abedi V, Mei Y, Hontecillas R, Hoops S, Carbo A, et al. Supervised learning methods in modeling of CD4+ T cell heterogeneity. BioData Min 2015;8:27.
[40] Goldberg E, Amir I, Zafran M, Gophna U, Samra Z, Pitlik S, et al. The correlation between Clostridium-difficile infection and human gut concentrations of Bacteroidetes phylum and Clostridial species. Eur J Clin Microbiol Infect Dis 2014;33:377–83.
[41] Rodriguez JM, Murphy K, Stanton C, Ross RP, Kober OI, Juge N, et al. The composition of the gut microbiota throughout life, with an emphasis on early life. Microb Ecol Health Dis 2015;26:26050.
[42] McKenney PT, Pamer EG. From hype to hope: the gut microbiota in enteric infectious disease. Cell 2015;163:1326–32.
[43] House TW. National Action Plan for Combating Antiobiotic-Resistant Bacteria; 2015.
[44] Buffie CG, Bucci V, Stein RR, McKenney PT, Ling L, Gobourne A, et al. Precision microbiome reconstitution restores bile acid mediated resistance to Clostridium difficile. Nature 2015;517:205–8.
[45] Abt MC, McKenney PT, Pamer EG. Clostridium difficile colitis: pathogenesis and host defence. Nat Rev Microbiol 2016;14:609–20.
[46] Voth DE, Ballard JD. Clostridium difficile toxins: mechanism of action and role in disease. Clin Microbiol Rev 2005;18:247–63.
[47] Cresci G, Nagy LE, Ganapathy V. Lactobacillus GG and tributyrin supplementation reduce antibiotic-induced intestinal injury. JPEN J Parenter Enteral Nutr 2013;37:763–74.
[48] Quesada-Gomez C, Lopez-Urena D, Chumbler N, Kroh HK, Castro-Pena C, Rodriguez C, et al. Analysis of TcdB proteins within the hypervirulent clade 2 reveals an impact of RhoA glucosylation on Clostridium difficile proinflammatory activities. Infect Immun 2016;84:856–65.
[49] Ng J, Hirota SA, Gross O, Li Y, Ulke-Lemee A, Potentier MS, et al. Clostridium difficile toxin-induced inflammation and intestinal injury are mediated by the inflammasome. Gastroenterology 2010;139:542–52, 552 e541-543.

[50] Naaber P, Mikelsaar RH, Salminen S, Mikelsaar M. Bacterial translocation, intestinal microflora and morphological changes of intestinal mucosa in experimental models of Clostridium difficile infection. J Med Microbiol 1998;47:591–8.
[51] Buffie CG, Bucci V, Stein RR, McKenney PT, Ling L, Gobourne A, et al. Precision microbiome reconstitution restores bile acid mediated resistance to Clostridium difficile. Nature 2014;517:205–8.
[52] Antharam VC, Li EC, Ishmael A, Sharma A, Mai V, Rand KH, et al. Intestinal dysbiosis and depletion of butyrogenic bacteria in Clostridium difficile infection and nosocomial diarrhea. J Clin Microbiol 2013;51:2884–92.
[53] Ozaki E, Kato H, Kita H, Karasawa T, Maegawa T, Koino Y, et al. Clostridium difficile colonization in healthy adults: transient colonization and correlation with enterococcal colonization. J Med Microbiol 2004;53:167–72.